IEEE Access
Multidisciplinary | Rapid Review | Open Access Journal

Received June 27, 2016, accepted July 15, 2016, date of publication July 21, 2016, date of current version September 28, 2016.

Digital Object Identifier 10.1109/ACCESS.2016.2593794

Small-Size Reconfigurable Loop Antenna for Mobile Phone Applications

HAO WANG[1], YIBO WANG[1], JIANLAN WU[2], PENG CHEN[1], ZHEQIANG WU[1], CHOW-YEN-DESMOND SIM[3], (Senior Member, IEEE), AND GUANGLI YANG[1]

[1]Key Laboratory of Specialty Fiber Optics and Optical Access Network, Shanghai University, Shanghai 200072, China
[2]College of Information and Communication Engineering, Harbin Engineering University, Harbin 150001, China
[3]Department of Electrical Engineering, Feng Chia University, Taichung 40724, Taiwan

Corresponding author: G. L. Yang (guangli.yang@shu.edu.cn)

This work was supported by the Shanghai 1000 Plan under Grant S.39-0107-14-201.

ABSTRACT A small-size reconfigurable loop antenna for mobile phone applications with a compact volume of $55 \times 5 \times 3$ mm^3 is proposed. In addition to the traditional three loop antenna modes, namely, 0.5-λ, 1-λ, and 1.5-λ modes, the proposed loop antenna also generates another 2-λ mode. To cover more operating bands with such compact antenna volume, the reconfigurable technique is therefore applied by inserting an RF switch at the end of the proposed antenna to improve bandwidth at the low band. By combining the four working states of RF switch, the proposed antenna can cover GSM850/900, DCS1800, PCS1900, UMTS2100, and LTE2300/2500 bands with low specific absorption rate and high efficiencies.

INDEX TERMS Mobile phone antenna, reconfigurable antenna, loop antenna, RF switch.

I. INTRODUCTION

With the increasing demand for ultra-thin smart phone, the ultimate challenge at the moment is to design a wideband antenna with very compact size/volume. Because the ultra-thin smart phone provides very limited available spaces for designing the required antenna, single passive and compact antenna usually has difficulty to support multiple bands and wide bandwidth enough to support all the required WAN bands for global applications. To resolve this issue, reconfigurable or active tunable antenna is one of the practical solutions to minimize antenna size [1]–[8]. The frequency configurability can be realized by using PIN diodes [1]–[4], digital tunable capacitors [5], or RF-MEMS (micro-electro mechanical systems) switches [6]–[8]. Determining which RF tunable technology to use depends on the antenna type, tuning range, harmonic side effect, RF component loss and other factors.

Besides PIFA (planar inverted F antenna), IFA (inverted F antenna) and monopole antennas, loop antenna is also a potential candidate for mobile phone applications because of its advantage of exciting multi-resonant modes. As reported in [9] and [10], 3-D type folded loop antenna can generate up to three resonant modes within the LTE bands of interest, namely, 0.5-λ, 1-λ and 1.5-λ modes. Recently, loop antennas with a higher 2-λ resonant mode have been studied [11]–[13]. As reported in [12], the higher 2-λ resonant mode is generated by the distance between the feed and shorting point of the loop antenna. However, the antenna size of [11]–[13] is fairly large at $50 \times 13 \times 5$ mm^3, $60 \times 8 \times 5$ mm^3 and $75 \times 10 \times 5$ mm^3, respectively. Therefore, they are not suitable for ultra-thin and narrow frame mobile phone applications.

In this paper, a small size ($55 \times 5 \times 3$ mm^3) internal loop antenna with multimode operation (up to four resonant modes) and frequency agility is proposed. A single-pole-four-throw RF switch (model RF-1604) is applied in this work for introducing four operation states so that the proposed antenna can operate at the desired bands. To further illustrate the merits of the proposed antenna, Table 1 shows the comparison between the proposed antenna and those loop antennas reported previously. Compared with the reference ones, this design method can significantly reduce the occupied volume. The obtained results show that the proposed antenna can give two wide frequency bands, in which the low band and high band are 780–990 MHz (210 MHz or 23.7%) and 1670–2740 MHz (1070 MHz or 48.5%), respectively. Thus, both low and high bands can cover the GSM850/900, DCS1800, PCS1900, UMTS2100, and LTE2300/2500 bands. In addition, the measured antenna efficiencies of low and high bands can be as high as 59% and 82%, respectively. To further study the effects of antenna radiation to human head at the transmit mode, the specific absorption rate (SAR) is also investigated. The simulated results show that the SAR

TABLE 1. Comparison between proposed antenna and reference antennas.

Antenna	Dimension(mm^3)	Bandwidth(MHz)	Efficiency(%)
[4]	60×5×5	790–980/ 1490–2565	>64.7/>47.4
[7]	30×10×5	704-960/ 1710-2690	30-62/58-73
[9]	60×15×4	824-960/ 1710-2170	>60/>66
[11]	50×13×5	698-960/ 1710-2170	>60/>73
[12]	60×8×5	800-1100/ 1700-2580	50-85/58-84
[13]	75×10×5	775-1100/ 1710-3020	>59
Proposed	55×5×3	780-990/ 1680-2740	50-59/52-82

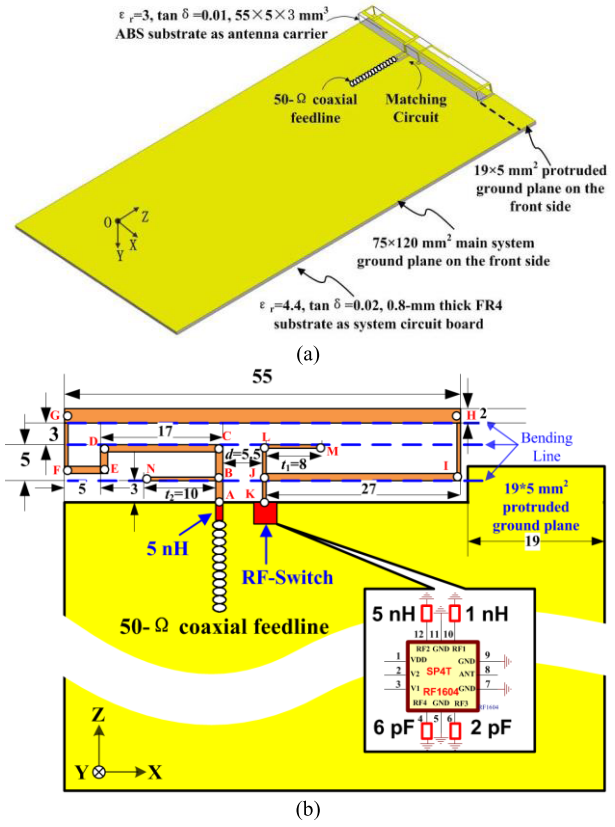

FIGURE 1. Geometry and detailed dimensions of proposed antenna. (a) Antenna geometry and PCB board, (b) Detailed dimensions of antenna and the structure of RF switch (unit: mm).

values of proposed antenna are well below the limit set by the federal communication committee (FCC).

II. ANTENNA STRUCTURE AND DESIGN PRINCIPALS

A. ANTENNA STRUCTURE

The configuration of proposed antenna is illustrated in Fig. 1. The overall geometry as shown in Fig. 1(a) indicates that the system circuit board of proposed antenna is built on a 0.8-mm thick FR4 substrate ($\varepsilon_r = 4.4, \tan\delta = 0.02$) with a planar size of 75 × 125 mm^2. On the top side of the FR4 substrate is a 75 × 120 mm^2 system ground plane printed with a protruded ground of 5 × 19 mm^2. Thus, a 5 × 56 mm^2 no-ground region can be observed on the left side of this protruded ground. Here, the protruded ground can be used for laying out electronic components such as metallic USB connector. A 3 mm thick ABS (Acrylonitrile Butadiene Styrene) substrate antenna carrier ($\varepsilon_r = 3, \tan\delta = 0.01$) is used to support the proposed antenna above the system circuit board, and a gap distance of 1 mm is set between the antenna carrier and the protruded ground plane. The total volume of radiating antenna element (built on the ABS) is only 55 × 5 × 3 mm^3, and it is located in the no-ground region.

The detailed planar dimensions of proposed antenna and the structure of RF switch are given in Fig. 1(b). The proposed antenna is composed of three branches, namely, branch #1 (a folded loop antenna along section A-B-C-D-F-G-H-I-J-K), branch #2 (section J-L-M) and branch #3 (section B-N). The folded loop section (branch #1) can excite four resonant modes for the bands of interest, and a few techniques are used to optimize the proposed antenna performances. Here, branch #2 and branch #3 are designed to achieve the high band operation bandwidth. To achieve good impedance matching, a series 5 nH inductor is loaded at the feed point as a matching component. For achieving frequency agility, the terminal end (point K) of branch #1 is linked to a SP4T (single-pole-four-throw) RF switch (model RF-1604), so that the low band from 780 to 980 MHz can be covered. From the magnified diagram of this RF switch shown in Fig. 1(b), four lumped components are linked to the four RF ports (RF1 to RF4). The RF switch states are controlled by two bias voltages (V1 and V2), and their corresponding truth table is given in Table 2.

TABLE 2. The truth table of the RF switch.

RF switch states	V1	V2	Output
State 1	0	0	1 nH
State 2	0	1	5 nH
State 3	1	0	2 pF
State 4	1	1	6 pF

B. OPERATION PRINCIPLE

To explain the antenna design principle, Fig. 2 shows the final simulated reflection coefficients of proposed antenna at different working states. The proposed loop antenna operates at the 0.5-λ, 1-λ, 1.5-λ and 2-λ modes by itself simultaneously where 0.5-λ is at low band and 1-λ, 1.5-λ and 2-λ modes at high band. To improve the 0.5-λ mode bandwidth, the SP4T RF switch with four states is used to cover 810-985 MHz for GSM 850/900 band operations. To make all the high band reflection coefficient under the VSWR of 3:1 to cover 1700–2830 MHz for DCS1800, PCS1900, UMTS2100 and LTE2300/2500 band application, branch #2 and 3 are applied for better impedance matching. Different from other loop antenna design [12], this antenna also generates the 2-λ resonant mode where the distance parameter ***d*** between the

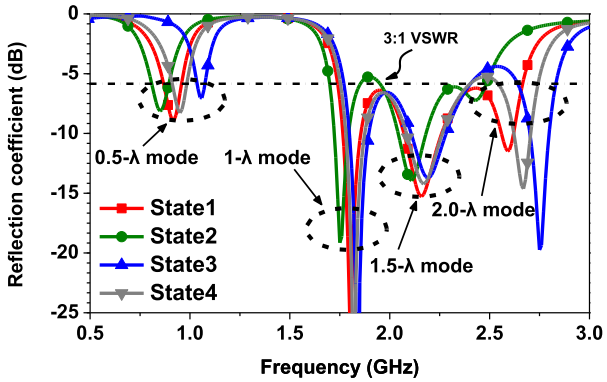

FIGURE 2. Simulated reflection coefficients of proposed antenna in four working states.

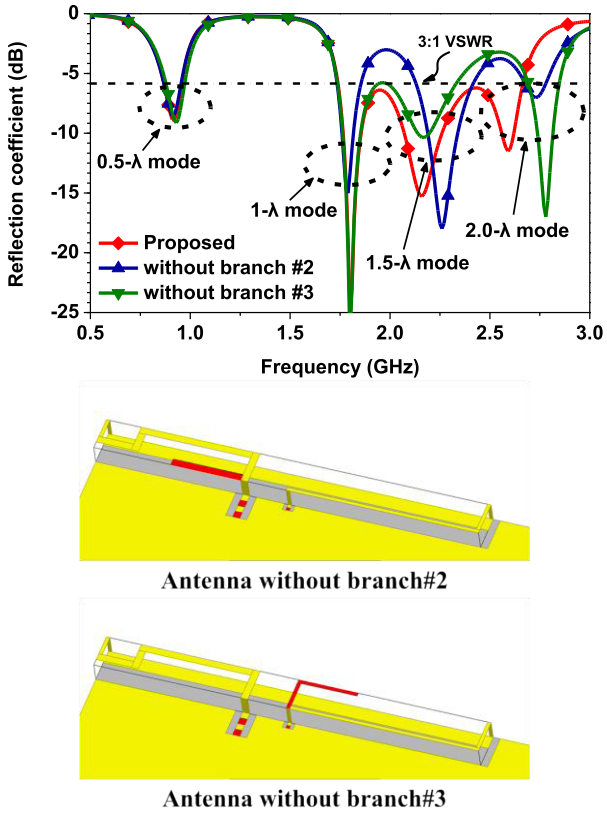

FIGURE 3. Simulated reflection coefficients of proposed antenna, the case without branch #2, and the case without branch #3 at State1 (1nH is on).

feeding line ABC and the grounding line KJL is critical for this mode.

To understand the functionalities of branch #2 and #3, Fig. 3 shows the simulated reflection coefficients of proposed antenna for the case without branch #2 and the case without branch #3 when the switch is at State 1 condition (1 nH is on). It is observed that, without branch #2, the 2-λ mode is shifted to higher frequency band; while in contrast, the 0.5-λ, 1-λ, and 1.5-λ resonant modes are only slightly affected. On the other hand, if branch #3 is removed from the proposed antenna, both 0.5-λ and 1-λ modes are only slightly deviated, and in contrast, the 1.5-λ and 2-λ modes are shifted to higher frequency band. Therefore, the main objective of adding branch #2 and branch #3 is to allow the proposed antenna to achieve enough bandwidths to cover the desired high band frequencies (1710–2690 MHz) for DCS1800, PCS1900, UMTS2100 and LTE2300/ 2500 band applications.

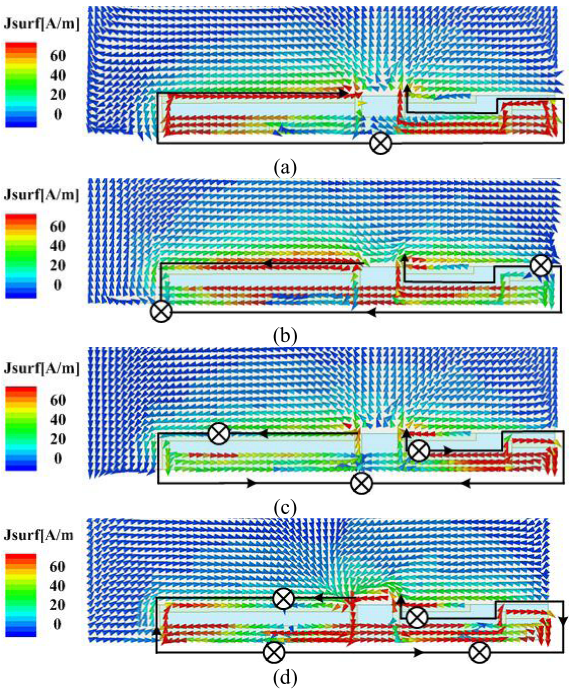

FIGURE 4. Simulated current distributions on metallic radiators and system ground of proposed antenna at State 1, (a) 900 MHz, (b) 1800 MHz, (c) 2100 MHz, (d) 2600 MHz. A cross within the circle indicates "null" point, and the arrow lines indicate the current paths.

To analyze the antenna's resonant modes more clearly, the simulated surface current distributions at 0.9 GHz, 1.8 GHz, 2.1 GHz and 2.6 GHz are plotted in Fig. 4. In this study, State1 is chosen for the evaluation (1nH is on). As shown in Fig. 4 (a), one current null is observed in the middle section of the loop antenna, and the current paths at both feed point and ground point are in the same direction. It can be explained that the loop antenna functions as a monopole antenna when it is at half wavelength long. So, this is a 0.5-λ or $2 \times 1/4$ λ monopole antenna mode. In [12], this is categorized as common mode. Note that the 0.5-λ mode or common mode is introduced from the function of the ground plane.

As shown in Fig. 4(b), there are two current nulls at the two sides of proposed antenna along the x-axis direction. Here, the current distributions at the feed point and ground point are in opposite directions, and the current path along the edge of the ground plane flows from the ground point to the feed point. Hence, it is clear that the proposed antenna operates at 1-λ loop antenna mode. In Fig. 4(c), three current nulls are indicated, and the current paths at the feed point and ground point are in the same direction. This is a 1.5-λ ($2 \times 3/4$ λ) monopole antenna mode. As depicted in Fig. 4(d), four

current nulls are observed, and the current paths at the feed point and ground point are in opposite directions, showing a current flow along the edge of the ground plane from the feed point to ground point. This indicates that the antenna operates at 2-λ loop antenna mode.

To conclude the analysis from Fig. 4: (I) The main current distribution path is the metallic loop strip (branch #1) from the feed point to ground point. (II) The current distributions in the two tuning branches (branch #2: section J-L-M, branch #3: section B-N) will change accordingly with different resonant modes. (III) Fig. 4 (a) and (b) show that the currents are weak in branch #2, but in Fig. 4(c) and (d), strong current distributions are observed along branch #2. This indicates that branch #2 mainly functions as a tuning branch at 1.5-λ and 2-λ mode. (IV) Branch #3 serves as a tuning branch at 1-λ, 1.5-λ and 2-λ modes, due to the strong current distributions at these modes.

C. PARAMETRIC STUDY

Several main parameters of proposed antenna are studied in this subsection. As mentioned before, the dimensions of the two tuning branches are important in achieving triple resonances to form wideband operation in the desired high band (1710–2690 MHz). To evaluate the function of tuning branch #2, the simulated reflection coefficient of proposed antenna at State 1 with different values of strip length t_1 of branch #2 is shown in Fig. 5. When t_1 is reduced from 12 mm to 4 mm (with a step decrement of 2 mm), both 1.5-λ mode and 2-λ mode are shifted to the higher frequency band, showing impedance mismatch for the 1.5-λ mode but better matching for 2-λ mode. In this case, both 0.5-λ and 1-λ modes remain almost the same. Hence, to combine the 1-λ, 1.5-λ and 2-λ modes together to cover the desired high band, the optimized length of t_1 is set to 8 mm.

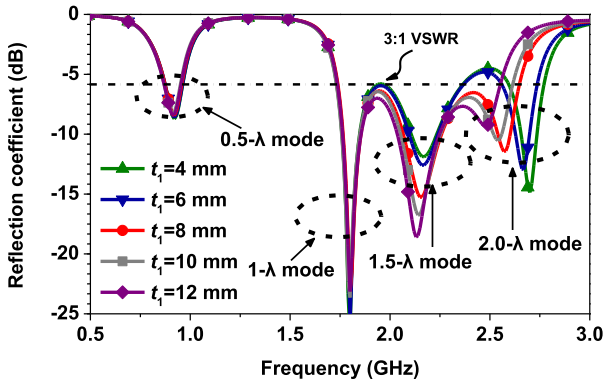

FIGURE 5. Simulated reflection coefficients with different values of t_1 in State 1.

As branch #3 is also an important element to achieve the desired high band coverage, Fig. 6 shows the simulated reflection coefficient with different values of strip length t_2 of branch #3. In this figure, when t_2 is decreased from 12 to 4 mm (with a step decrement of 2 mm), both 1.5-λ and 2-λ modes are shifted to the higher frequency band.

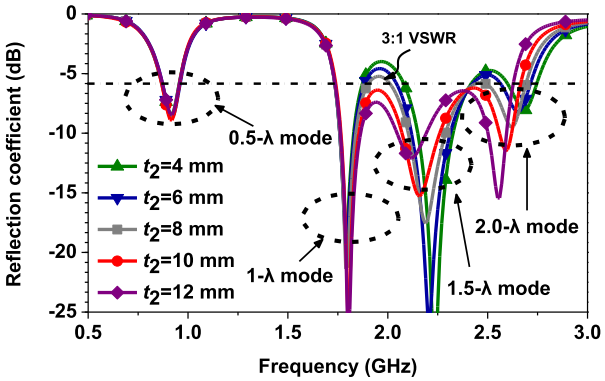

FIGURE 6. Simulated reflection coefficients with different values of t_2 in State 1.

Meanwhile, the 1-λ mode is slightly affected, and the 0.5-λ mode remains almost the same. Hence, to achieve wide operating band and good impedance matching in the desired high band, the length t_2 is optimized to 10 mm.

One of the unique features of this 3-D loop antenna is that a higher 2-λ mode can be excited in addition to the traditional 0.5-λ, 1-λ and 1.5-λ resonant modes. As discussed earlier, the parameter gap length d (the distance between the feeding section ABC and the grounding section KJL) is critical to the generation of the higher 2-λ mode. To illustrate how this 2-λ mode is excited, the simulated reflection coefficients as a function of the gap distance d are shown in Fig. 7. In this figure, it is realized that decreasing d from 20.5 mm to 0.5 mm (with a step decrement of 5 mm) will result in shifting all the four resonant modes to the lower frequency band. It is also noteworthy that when a large gap distance is applied ($d = 20.5$ mm), the 2-λ mode is at frequency > 3 GHz with very undesirable impedance matching. Here, the gap distance d has been optimized to 5.5 mm to achieve good low and high band operations.

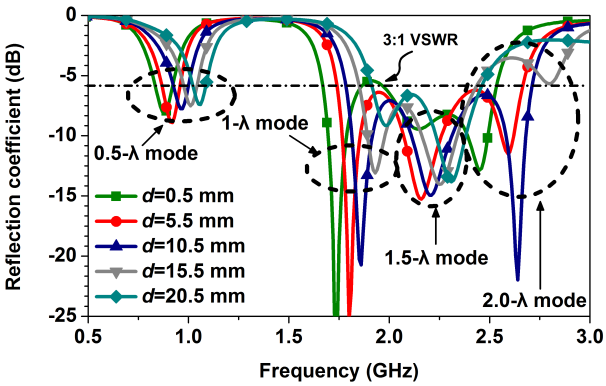

FIGURE 7. Simulated reflection coefficients with different values of d in State 1.

III. RESULTS AND DISSCUSSION

A. FREE SPACE

The proposed antenna was fabricated and tested. Fig. 8 shows the photograph of the fabricated antenna prototype. To verify

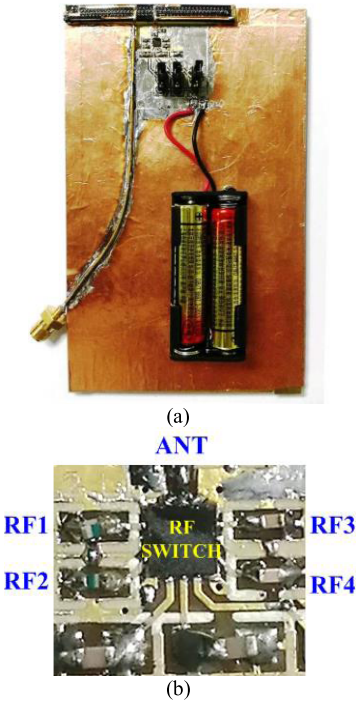

FIGURE 8. (a) Photo of the fabricated reconfigurable antenna (b) photo of the RF switch.

the reconfigurable mechanism of the proposed 3-D type loop antenna, a SP4T RF switch (RFMD RF1604) was applied in the designed PCB (printed circuit board). As no external DC blocking capacitors are required on RF ports due to the internal port integration, thus, the RF switching circuit is simplified. As depicted in TABLE II, the ANT port is connected to the K point of loop antenna, and RF1 to RF4 ports are connected to a single chip component with value of 1 nH, 5 nH, 2 pF and 6 pF, respectively. The switching of the four working states can be realized by controlling the biasing voltages on the V1 and V2 pins. Two AA batteries were used to supply 3-V voltage for the RF switch.

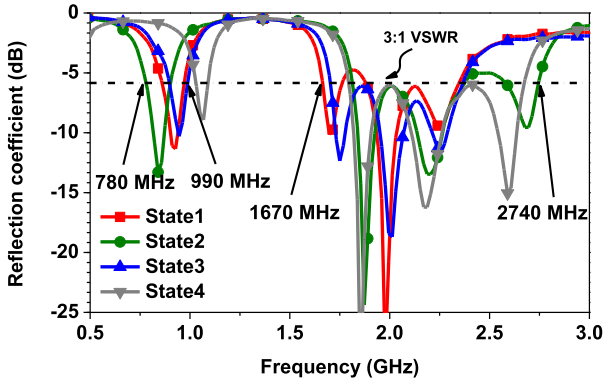

FIGURE 9. Measured reflection coefficients of the proposed antenna.

The measured reflection coefficients of the proposed antenna with the RF switching circuit are presented in Fig. 9. The measured low band reflection coefficients agreed well with the simulation ones in Fig. 2. As for the measured high band reflection coefficients, the higher resonant modes are slightly different from the simulation shown in Fig. 2. This is mainly owing to the parasitic inductance from the RF switch which induced additional electrical length that results in shifting the high band resonances to the lower frequency band. Furthermore, because the effects of RF switch are not taken into account during the simulation, therefore, the lumped components that are linked directly at the end of the loop strip (K point) may also contribute to the differences between measurement and simulation.

When switched to State1, the measured operating bandwidths (at VSWR 3:1) were 860–970 MHz, 1670–1755 MHz and 1890–2380 MHz. At State 2, the measured bandwidths were 780–900 MHz, 1810–2380 MHz and 2590–2740 MHz. As for State 3, the measured bandwidths were 1020–1095 MHz and 1795–2690 MHz, and for State 4, the measured bandwidths were 900–990 MHz and 1710–2365 MHz. Therefore, by combing all the four working states, the achieved desirable operating bandwidths in the low and high bands are 780–990 MHz and 1670–2740 MHz, which can cover the GSM850/900, DCS1800, PCS1900, UMTS2100, and LTE2300/2500 bands for hepta band WWAN/LTE operations.

The far-field radiation patterns of proposed antenna were measured in a standard ETS AMS 8500 chamber. Fig. 10 shows the measured 2-D radiation patterns at 0.9 GHz (State 1), 1.82 GHz (State 2), 2.2 GHz (State 2) and 2.6 GHz (State 3). The radiation pattern at 0.9 GHz in the x-y plane has exhibited the bi-directional pattern that is related to a half-wave dipole resonant mode. The obtained radiation patterns are similar to the radiation patterns in modern mobile phone antennas.

The measured antenna efficiencies and gains of the four working states are shown in Fig. 11. The insertion loss of the RF switch is also taken into consideration. Within the desired GSM850/900 band (824–960 MHz), the measured gains and antenna efficiencies were -0.26–0.47 dBi and 50%–59%, respectively. As for its corresponding desired high band operation for DCS1800, PCS1900, UMTS2100, and LTE2300/2500 bands (1710–2690 MHz), the measured gains and efficiencies were 0.98–2.74 dBi and 51%–82%, respectively. The measured efficiencies and gains of the proposed antenna are feasible for practical mobile phone application.

B. SAR PERFORMANCE

To verify the antenna radiation to human body, the SAR simulation model was studied and performed based on the FCC standard, as shown in Fig.12. Here, the simulated SAR values for 1-g and 10-g head tissues are given in Table 3. The system circuit board is placed near the ear of the head phantom with a gap distance of 5 mm, and it is inclined 60^{o} with respect to the vertical line. The simulated 1-g and 10-g SAR values at 859, 925, 1795, 1920, 2045, 2350

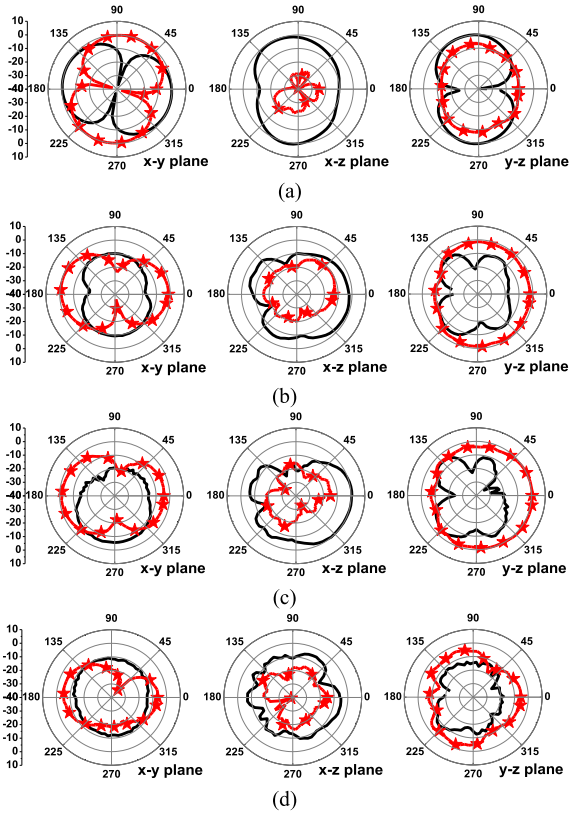

FIGURE 10. Measured radiation patterns, (a) 0.9 GHz (State 1), (b) 1.82 GHz (State 2), (c) 2.2 GHz (State 2), and (d) 2.6 GHz (State 3). (—— E_θ, —★— E_φ; unit: dBi).

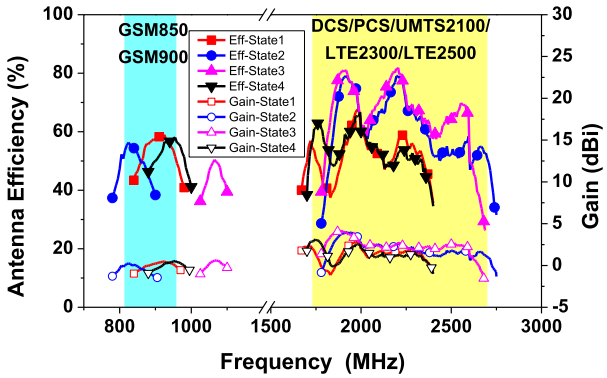

FIGURE 11. Measured peak gains and antenna efficiencies across all the bands of interest.

and 2595 MHz are all listed in Table 3. The input power for SAR simulation is 24 dBm or 0.2512 W for 859 and 925 MHz, and 21 dBm or 0.1256 W for 1795, 1920, 2045, 2350 and 2595 MHz. The corresponding simulated S11 and efficiencies are given at free space and phantom head case, respectively. The simulated total efficiencies at phantom head case are all over 40%. The obtained SAR values are under the SAR limit of 1.6 W/kg for 1-g tissue and 2.0 W/kg for 10-g tissue, which are acceptable for practical mobile application.

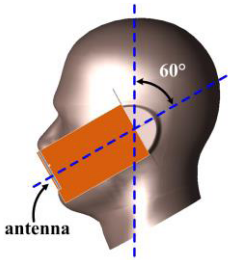

FIGURE 12. SAR simulation model for the proposed antenna.

TABLE 3. SAR values for 1-g and 10-g head tissues.

Frequency (MHz)		859	925	1795	1920	2045	2350	2595
Input power (dBm)		24	24	21	21	21	21	21
1-g SAR (W/kg)		0.64	0.67	0.16	0.13	0.47	0.49	0.28
10-g SAR (W/kg)		0.47	0.48	0.10	0.08	0.31	0.30	0.16
S11 (dB)	free space	-8.0	-8.9	-18.6	-8.1	-9.8	-7.3	-11.5
	with head	-8.8	-9.7	-15.3	-4.8	-5.6	-6.0	-6.9
Effi-cien-cy (%)	free space	60	63	78	55	59	62	55
	with head	42	43	69	48	43	44	44
Resonant Mode		0.5-λ		1-λ		1.5-λ		2-λ

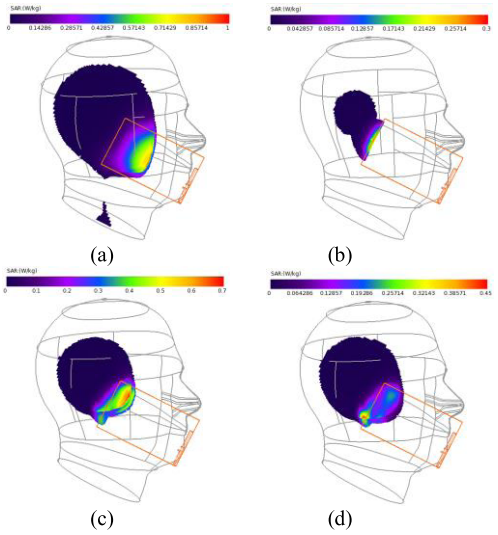

FIGURE 13. Simulated maximum SAR value at different modes (a) 0.925 GHz of 0.5-λ mode, (b) 1.92 GHz of 1.0-λ mode, (c) 2.35 GHz of 1.5-λ mode, (d) 2.595 GHz of 2.0-λ mode.

To better understand the SAR distribution inside phantom head, the simulated SAR density distributions at four resonant modes are presented in Fig.13.

IV. CONCLUSION

A small-size reconfigurable loop antenna for mobile application has been successfully demonstrated. The proposed antenna has a compact volume of 55 × 5 × 3 mm^3.

It consists of a folded loop structure, two tuning branches and an RF switch. The loop structure itself can generate one resonant mode for the low band, and three resonant modes for the high band. The two tuning branches used in this work are to slightly tune the high band, and an RF switch is applied to improve the low band operating bandwidth with four states. The proposed antenna can cover 780–990 MHz and 1680–2740 MHz by switching between the four states. The average efficiency is over 50% at low band and 52% at high band. The simulated SAR value is much less than the 1.6 W/kg for the 1-g head tissue. Based on the desirable antenna performances with compact size, this proposed antenna is a good candidate for slim smart phone applications.

REFERENCES

[1] S. W. Lee, H. S. Jung, and Y. J. Sung, "A reconfigurable antenna for LTE/WWAN mobile handset applications," *IEEE Antennas Wireless Propag. Lett.*, vol. 14, pp. 48–51, Jan. 2015.

[2] S. W. Lee and Y. Sung, "Compact frequency reconfigurable antenna for LTE/WWAN mobile handset applications," *IEEE Trans. Antennas Propag.*, vol. 63, no. 10, pp. 4572–4577, Oct. 2015.

[3] Y.-L. Ban, Z. X. Chen, Z. Chen, K. Kang, and J. L.-W. Li, "Reconfigurable narrow-frame antenna for heptaband WWAN/LTE smartphone applications," *IEEE Antennas Wireless Propag. Lett.*, vol. 13, pp. 1365–1368, Jul. 2014.

[4] Y. Li, Z. Zhang, J. Zheng, Z. Feng, and M. F. Iskander, "A compact hepta-band loop-inverted F reconfigurable antenna for mobile phone," *IEEE Trans. Antennas Propag.*, vol. 60, no. 1, pp. 389–392, Jan. 2012.

[5] W.-W. Lee and Y.-S. Cho, "Frequency tunable antenna using coupling patterns for mobile terminals," *Electron. Lett.*, vol. 51, no. 22, pp. 1725–1726, Oct. 2015.

[6] X. Meng, "Small-size eight-band frequency reconfigurable antenna loading a MEMS switch for mobile handset applications," *Int. J. Antennas Propag.*, vol. 2014, May 2014, Art. no. 143415.

[7] C.-H. Chang, S.-Y. Huang, W.-C. Wei, and P.-J. Ma, "Small-size adjustable LTE/WWAN coupled-fed loop antenna for mobile handset applications," *Microw. Opt. Technol. Lett.*, vol. 56, no. 11, pp. 2687–2691, Nov. 2014.

[8] Y.-L. Ban, S.-C. Sun, P.-P. Li, J. L.-W. Li, and K. Kang, "Compact eight-band frequency reconfigurable antenna for LTE/WWAN tablet computer applications," *IEEE Trans. Antennas Propag.*, vol. 62, no. 1, pp. 471–475, Jan. 2014.

[9] K.-L. Wong and C.-H. Huang, "Printed loop antenna with a perpendicular feed for penta-band mobile phone application," *IEEE Trans. Antennas Propag.*, vol. 56, no. 7, pp. 2138–2141, Jul. 2008.

[10] K.-L. Wong and M.-T. Chen, "Small-size LTE/WWAN printed loop antenna with an inductively coupled branch strip for bandwidth enhancement in the tablet computer," *IEEE Trans. Antennas Propag.*, vol. 61, no. 12, pp. 6144–6151, Dec. 2013.

[11] M. Zheng, H. Wang, and Y. Hao, "Internal hexa-band folded monopole/dipole/loop antenna with four resonances for mobile device," *IEEE Trans. Antennas Propag.*, vol. 60, no. 6, pp. 2880–2885, Jun. 2012.

[12] D. Wu, S. W. Cheung, and T. I. Yuk, "A compact and low-profile loop antenna with multiband operation for ultra-thin smartphones," *IEEE Trans. Antennas Propag.*, vol. 63, no. 6, pp. 2745–2750, Jun. 2015.

[13] H. Xu *et al.*, "A compact and low profile loop antenna with six resonant modes for LTE smartphone," *IEEE Trans. Antennas Propag.*, to be published.

HAO WANG was born in Jiangsu, China, in 1992. He received the B.S. degree in communication engineering from Shanghai University, China, in 2014. He is currently pursuing the M.S. degree with Shanghai University, China. His main research interests are reconfigurable antennas for mobile terminal application and short range FMCW radar.

YIBO WANG received the B.S. degree from the Shanghai University of Electric Power, China, in 2014. He is currently pursuing the M.S. degree in electrical engineering with Shanghai University, China. His current research interests include small sized antennas and phased array for the applications of the next generation (5G) wireless communications.

JIANLAN WU was born in Shanxi, China, in 1995. She received the degree from the College of Information and Communication Engineering, Harbin Engineering University in 2013. Her main interest is electronic information engineering.

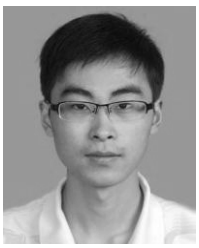

PENG CHEN was born in Jiangsu, China, in 1991. He is currently pursuing the M. S. degree with Shanghai University. His interests include antennas for FMH devices and reconfigurable antennas.

ZHEQIANG WU was born in Hubei, China, in 1990. He received the B.S. degree in communication engineering from Shanghai University, China, in 2014. He is currently pursuing the M.S. degree with Shanghai University, China. His main research interest is MIMO antenna for handset terminal.

CHOW-YEN-DESMOND SIM (M'07–SM'13) was born in Singapore, in 1971. He received the B.Sc. degree from the Engineering Department, University of Leicester, U.K., in 1998, and the Ph.D. degree from the Radio System Group, Engineering Department, University of Leicester, in 2003. From 2003 to 2007, he was an Assistant Professor with the Department of Computer and Communication Engineering, Chienkuo Technology University, Changhua, Taiwan. In 2007, he joined the Department of Electrical Engineering, Feng Chia University (FCU), Taichung, Taiwan, as an Associate Professor, where he became a Full Professor in 2012. He is currently the Executive Officer of Master's Program with the College of Information and Electrical Engineering (Industrial Research and Development), the Director of Intelligent IoT Industrial Ph.D. Program, and the Director of the Antennas and Microwave Circuits Innovation Research Center with FCU. He has authored or coauthored over 80 SCI papers. His current research interests include antenna design, VHF/UHF tropospheric propagation, and RFID applications. He is a fellow of the Institute of Engineering and Technology, a Senior Member of the IEEE Antennas and Propagation Society, and a Life Member of the IAET. In 2015, he was invited to become the Distinguished Chair Professor (ZiQiang Professor) with the School of Communication and Information Engineering, Shanghai University. He was the TPC Member of the APMC 2012, the APCAP 2015, and the IMWS-Bio 2015. He served as the TPC Sub-Committee Chair (Antenna) of the ISAP 2014. He was a recipient of the IEEE Antennas and Propagation Society Top ten Outstanding Reviewer Award for Year (2013/2014), (2014/2015), and (2015/2016). He received the fee waiver Ph.D. Scholarship from the Radio System Group, Engineering Department, University of Leicester, in 1999. He was invited as the Workshop Speaker in APEMC 2015 and ICAT 2016, and the Invited Speaker of TDAT 2015. He serves as the TPC Chair of the APCAP 2016 and the Chapter Chair of the IEEE AP-Society, Taipei Chapter (from 2016 to 2018).

GUANGLI YANG received the B.S. degree in physics from the Beijing University of Science and Technology, China, in 1997, and the Ph.D. degree in electrical engineering from the University of South Carolina, USA, in 2005. He was mostly with antenna and RF research group in Motorola Inc., USA, from 2005 to 2013 started as a Senior, a Senior Staff, and promoted to Principal Engineer before left the company. He had been a Professor with Shanghai University Since 2014. He has authored or co-authored over 20 publications and has over 14 patents filed or issued. His research interests include smart antennas, antenna miniaturization and configurability, digital beam-forming system, and microwave circuits. He is currently the Director of the RF Research Group at Shanghai University and a recipient of Shanghai 1000 Plan and Eastern Scholarship Awards in 2013.